

08,03

Revisiting the fine structure of $2p$ spectra from the (100) silicon surface

© M.V. Kuzmin, A.A. Monyak, S.V. Sorokina

Ioffe Institute,
St. Petersburg, Russia
E-mail: m.kuzmin@mail.ioffe.ru

Received May 22, 2024

Revised May 22, 2024

Accepted May 24, 2024

Using the synchrotron radiation and high-resolution photoelectron spectroscopy (56–66 meV), the fine structure of the $2p$ spectra from the Si(100) surface at 100 K has been studied in a wide range of electron escape depths. It is shown that these spectra include five surface components. The relationship between their core-level shifts and the atomic and electronic structure of the $c(4 \times 2)$ reconstruction is established. The experimental conditions where the $2p$ spectra have the greatest sensitivity to the surface and bulk of silicon are determined and, in particular, the inelastic mean free path for electrons in a silicon crystal is obtained as a function of photon energy. The results obtained can be used as reference data in studies of various surface structures on the Si(100) substrate using photoemission techniques.

Keywords: surface, photoelectron spectroscopy, core level, surface shift, silicon, inelastic mean free path.

DOI: 10.61011/PSS.2024.07.58994.132

1. Introduction

Photoelectron spectroscopy of core levels (PES-CL) is one of most informative methods of surface atomic structure study [1–3]. Using it the energy shifts of internal shells of surface atoms, or *surface shifts*, determining both difference of kinetic energy of electrons escaping volume and surface of sample. This difference arises because the positions of these shells are sensitive to the chemical and coordination environment of the atom. Hence, studying thin structure of PE-spectra of CL we can obtain information on nature of bonds and charge state of atoms in surface reconstructions, at interfaces and in different thin-film structures.

During last decades in literature a great amount of results occurred, they were obtained using PES-CL of high resolution for film systems metal-semiconductor and dielectric-semiconductor. A little portion of them, for example, was discussed in review [4]. Apparently, that to such results explanation requires detail understanding of form of spectral lines and nature of CL shifts for clean surfaces of semiconductors. However, even in this case, the interpretation of the fine structure of the PE spectra is far from completion. In particular, there is no agreement in the interpretation of the results for the Si(100) face, which is one of the most thoroughly studied semiconductor surfaces. In earlier papers in its $2p$ -spectra the surface component was detected, shifted by 0.5 eV to region of low bond energies [5–9]. It was interpreted as emission from top layer atoms surface (dimers) of reconstruction (2×1). Further use of PES-CL with high resolution gave possibility to determine four surface components in $2p$ -spectra of reconstructions Si(100) $c(4 \times 2)$ at 120 K and Si(100)(2×1) at 300 K [10]. Two of them were bonded with atoms of axisymmetric dimers in first layer (atoms $1u$

and $1d$ in Figure 1). Their surfaces shifts are -0.485 and 0.062 eV respectively. Additional two surface components were attributed to atoms of second layer (atoms 2 in Figure 1) and half of atoms of third layer. Their shifts are 0.22 and -0.205 eV, respectively.

Alternative interpretation of $2p$ -spectra of Si(100) face was presented in paper [12]. Its authors set in compliance with atoms $1d$ the component with surface shift 0.278 eV. At the same time the surface shifts 0.138 and -0.200 eV were attributed respectively to atoms of below located layer and atoms of first layer forming symmetric dimers. Besides, in paper [12] two additional features were identified in $2p$ -spectra shifted to region of somewhat higher energies. They were interpreted as surface and volume peaks of characteristic losses. Similar features were observed in the paper [13]. The authors of this study associated their appearance with surface defects and characteristic energy losses for interband transitions between two surface states near the band gap of silicon.

One more interpretation of surface shift for Si(100) was suggested in article [14]. The authors identified six surface components, explanation was provided for four components only. According to this article the component shifted by 0.13 eV to region of high energies is determined by atoms $1d$ and $4'd$ in Figure 1. Components with shifts 0.22 and -0.22 eV originated from atoms of third and fourth layers. At the same time emission from atoms of second layer does not result in occurrence of individual surface component in $2p$ -spectra, but contributes to bulk component.

Note also that in considered studies there are other differences. In particular, in them during decomposition of $2p$ -spectra different values of Lorentzian width (ω_L) were used. It varies from 46 meV in paper [14] to 85 meV in [10].

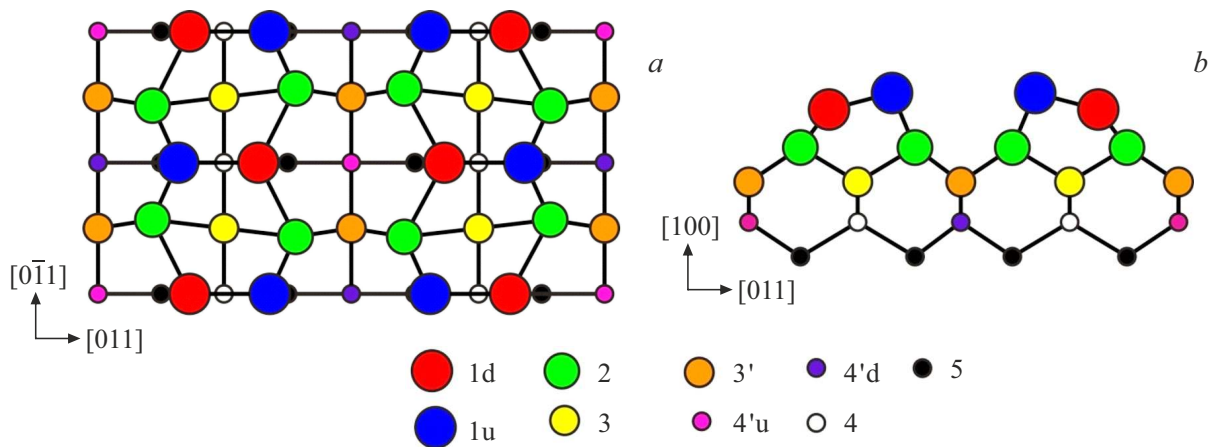


Figure 1. Atomic structure of surface Si(100)c(4 × 2): *a* — top view, *b* — side view. In bottom designations of atoms in different layers are given. Model is adapted from paper [11].

Apparently, the selection of this and other parameters of decomposition indicates significant effect on accuracy and reliability of the results.

Based on all stated above the objective is set to perform in this paper more reliable analysis of the fine structure of $2p$ -spectra for surface (100) of silicon. Several conditions were met for this. Firstly, the measurements were carried out at low temperature (100 K) and high energy resolution. Secondly, $2p$ -spectra were registered at different values of photon energies ($h\nu$) and angles (θ_e) of electrons escape from surface. This ensured varying of free run length and escape depth of electrons in wide range. Thirdly, during experiments high degree of purity and structural imperfection of surface Si(100) was ensured. All this made it possible to obtain detailed information about the shape of the spectral line of clean Si(100) surface. The article then briefly describes the experimental procedure and presents the main results of the study.

2. Experimental procedure

Experiments were performed in channel I4 of synchrotron MAX-lab (accumulating ring MAX-III) in Lund (Sweden). Spectra of $2p$ -level of silicon are registered using analyzer SPECS Phoibos 100 at temperature 100 K and residual pressure in vacuum chamber $3 \cdot 10^{-11}$ Torr. Full energy resolution was 56–66 meV depending on selected energy of quanta $h\nu$ (it changes in range 108–145 eV). To determine the resolution, and to calibrate scale of energy PE-spectra were used of edge of valence band of tantalum tape, which was preliminary thoroughly cleaned in oxygen and was in electric contact with Si sample. Angle of emission θ_e was counted relative to normal to surface and changed from 0° to 80° . The solid angle of electrons gathering was $\pm 1^\circ$.

As samples the targets with size $10 \times 5 \times 0.3$ mm were used, they were prepared from plate of single crystal silicon

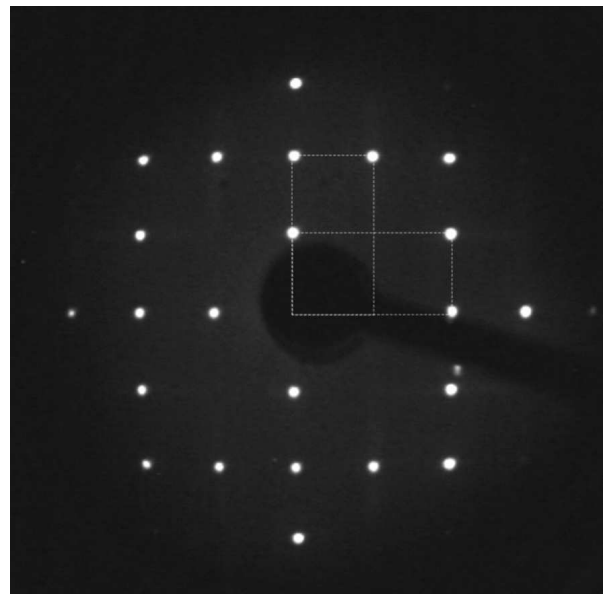


Figure 2. Diffraction pattern on surface Si(100) at room temperature. Dashed lines show two mutually orthogonal lattice cells of structure (2 × 1). Electron energy is 95 eV.

with surface orientation (100), doped with phosphorous (*n*-type), with resistivity $\sim 5 \Omega \cdot \text{cm}$. For their surface cleaning series of short heatings at 1530 K was used, when pressure in vacuum chamber increased above $1 \cdot 10^{-9}$ Torr. Then sample temperature quickly decreased to 1250 K and held at this value for some time to smooth the atomic steps on the surface. After cooling to room temperature clear diffraction pattern (2 × 1) was observed with bright reflexes and low level of background (Figure 2). Further the crystal was cooled to 100 K. On its surface structure c(4 × 2) was formed (Figure 1). Then PE-spectra were registered.

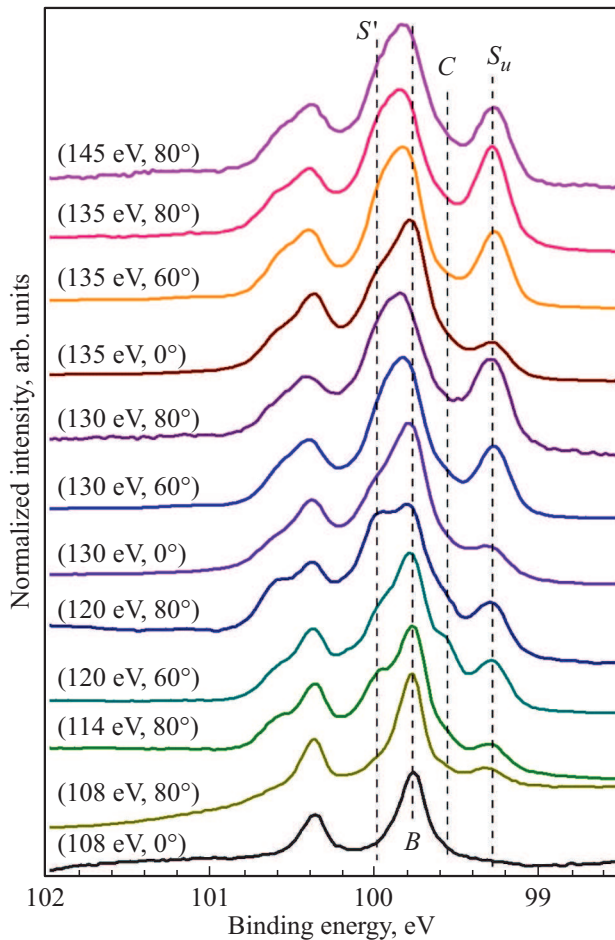


Figure 3. Normalized spectra of surface Si(100)c(4 × 2) at different experimental conditions ($h\nu$, θ_e). The bond energy was read from the Fermi level. Dashed lines indicate position of different components.

3. Results and discussion

Figure 3 shows a series of normalized $2p$ -spectra of surface Si(100)c(4 × 2), obtained at different values $h\nu$ and θ_e . Even without decomposition we can identify in them some important features indicating the energy position of some components (spin-orbital doublets). Spectrum registered at $h\nu = 108$ eV and $\theta_e = 0^\circ$ corresponds to maximum in this study escape depth of electron (kinetic energy ~ 3 eV) from crystal. Apparently, the main contribution to it is made by atoms of bulk lattice. This ensures determination of approximate position of the doublet B , determined by the emission from bulk of silicon. Energies of its $2p_{1/2}$ - and $2p_{3/2}$ -sublayers are approximately equal to 100.37 and 99.77 eV.

As values $h\nu$ and θ_e increase the escape depth decreases, and in spectra new features appear, which are determined by atoms of surface reconstruction c(4 × 2) and appropriate spin-orbital doublets shifted to region of larger or lower energies relative to B . So, the most obvious surface component is doublet S_u . The position of its $2p_{3/2}$ -sublayer

corresponds to maximum with energy 99.28 eV. This peak practically is not overlapped with rest portion of spectrum.

Two other surface components, which can be qualitatively observed in spectra in Figure 3, are doublets S' and C . First of them is most clearly visible at quantum energies $h\nu = 114$ and 120 eV. It is shifted towards larger energies relative to B by about 0.2–0.25 eV. Presence of the doublet C can be determined by occurrence of a small branch in region of energy 99.56 eV in spectrum at $h\nu = 120$ eV and $\theta_e = 60^\circ$. Its shift is about 0.2 eV.

To obtain more detail information $2p$ -spectra with quantitatively decomposed to components using the method of least-squares. Background was abstracted using Shirley method [15]. In decomposition the linear combination of the Voigt reference functions being a convolution of the Gaussian and Lorentzian line forms was used. Some adjustable parameters — Lorentzian width ω_L , spin-orbit splitting (0.610 eV) and ratio of intensities of $2p_{1/2}$ - and $2p_{3/2}$ -sublayers (1:2) — were same for all components and don not vary during adjustment. It is known that value ω_L (natural line breadth) is due to finite life time of the atom in photoexcited state with a hole on CL [16]. It depends on environment of atoms in silicon crystal and shall be same for all components in decomposition. But, in literature, as specified in Section 1, there is no consensus on what its value is optimal for $2p$ -spectra Si(100). In present paper the authors try to solve this problem. Figure 4 shows that Lorentzian affects the quality of representation of $2p$ -spectrum. In it for different values ω_L the difference spectra are presented, obtained by subtraction of the adjustment result from experimental data. It is evident that at low values ω_L (40–55 meV) the low energy part of spectra near energy 99 eV is poorly represented. When value ω_L increases the quality of adjustment in this energy region is improved. But at the same time accuracy of spectra representation at energies 99.3–100.6 eV decreases. Especially large residue in this region is observed at $\omega_L = 85$ –100 meV. From these results we can conclude that optimal value of Lorentzian width for $2p$ -spectra of surface Si(100) is $\omega_L = 70$ meV. This value was used in the further described decomposition

Other adjustable parameters were varied. They include number of components, their Gaussian width (ω_G), intensity and position on energy scale. Value ω_G is determined both by the energy resolution (instrumental resolution plus thermal broadening of lines), and the degree of local disordering of the crystal structure of the sample. Since the local inhomogeneity of the crystal lattice sites can differ significantly for different layers of atoms, the Gaussian, along with the surface shifts, contains important information about the atomic structure of the surface.

The decomposition results are presented in Figure 5. The round symbols in it show the experimental data, and the solid lines show the adjustment results. The spectra contain bulk component B and five surface components S_u , S_d , S' , C and D . Their surface shifts and Gaussian width are shown in Table 1. Use in the decomposition of

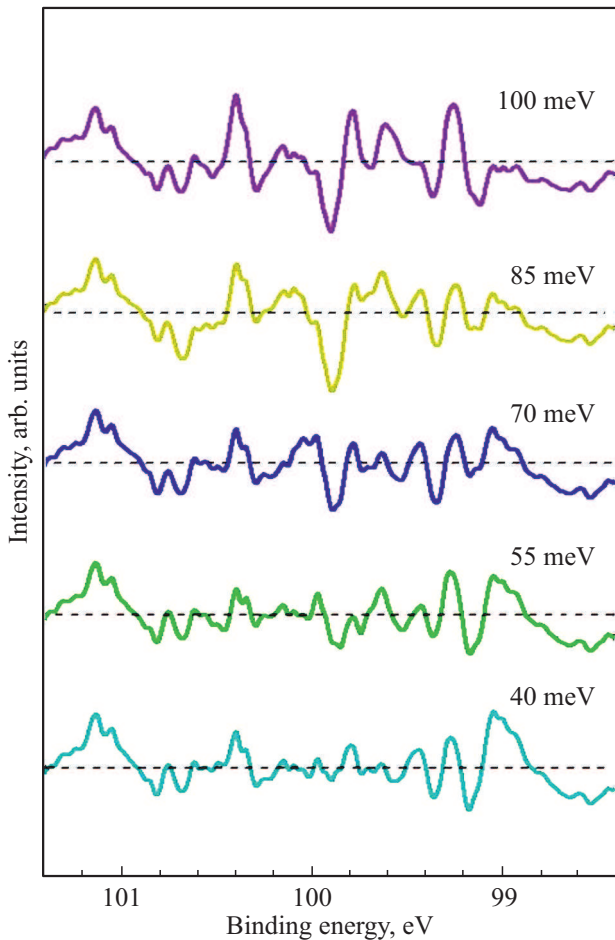


Figure 4. Difference spectra for different values of parameter ω_L . Decompositions were performed for $2p$ -line at $h\nu = 135$ eV and $\theta_e = 80^\circ$. Dashed lines indicate level where residue is zero.

four surface components (without D) in principle ensures satisfactory representation of individual spectra in Figure 5. But in this case the surface shifts would depend on the experimental conditions ($h\nu$ and θ_e), which has no physical sense. Besides, such decomposition scheme die not allow rather accurate representation of high energy part of some spectra. Hence, it can not be accepted for spectra in Figure 5. On the other hand, introduction of additional, six, surface component did not gave any improvement of adjustment quality. Based on this the decomposition scheme with six surface components was also negated. So, the results obtained in this paper did not confirm the presence of six surface component with shift 1.4 eV, observed for Si(100) in papers [12–14]. Obviously, this component was due to features of experiment in said studies.

Analysis of the results in Figure 5 allows us to draw a number of conclusions regarding the properties of $2p$ -line and nature of its components. From this it follows that upon change of escape depth the contribution of different doublets into the full intensity of spectra can vary in wide ranges. Figure 6, *a* shows such dependences for the case

Table 1. Surface shifts and Gaussian width for different components in $2p$ -spectra of surface Si(100)c(4×2)

Component	Surface shift (eV)	Gaussian width (eV)
B	–	0.143 ± 0.014
S_u	-0.483 ± 0.004	0.208 ± 0.014
S_d	0.078 ± 0.015	0.204 ± 0.016
S'	0.225 ± 0.014	0.159 ± 0.021
C	-0.163 ± 0.005	0.256 ± 0.016
D	0.320 ± 0.016	0.233 ± 0.042

$\theta_e = 80^\circ$. It shows in percent ratio the contributions of components B , S_u , S_d , S' , C and D into the full intensity of spectra during different photon energies $h\nu$. On top in graph along the horizontal axis also values of kinetic energies of electrons are shown. For even greater clarity, these curves can be modified depending on the normalized intensity S_u , S_d , S' , C and D (normalization is performed by value of component B) on photon energy (Figure 6, *b*). Both Figures show that contribution of emission from atoms of bulk lattice into spectra is minimum at $h\nu \cong 135$ eV (kinetic energy of electrons ≈ 30 eV). At this photon energy the spectra are most surface sensitive. When values $h\nu$ increase or decrease the surface sensitivity of spectra decrease, and their bulk sensitivity increases.

For components S_u and S_d the reverse, almost mirror situation is observed. At $h\nu \cong 135$ eV their contribution into PE-line is maximum. Upon increase or decrease of the photon energy the intensities S_u and S_d abruptly decrease, at that by area these doublets during all experimental conditions stay approximately equal to each other. Such behavior of components S_u and S_d is explained by that they are due to emission from atoms of top layer ($1u$ and $1d$ in Figure 1 respectively). This layer is formed by asymmetric, inclined to surface plane dimers Si($1d$)-Si($1u$), and charges localized on heir bottom and top ends are different [17,18]. flow of electronic density in this dimer occurs from the atom $1d$ to $1u$. This determines the energy splitting of $2p$ -level of atoms Si of top layer into two doublets in PE-line, and determines values of surface shifts of components S_d and S_u .

Also note that the shifts of the components considered are in good agreement with the results of *ab initio* calculations carried out on the basis of density functional theory [11,14,19,20]. Theoretical shift for atom $1u$ in different papers varies from -0.35 to -0.24 eV in initial state model and from -0.54 to -0.48 eV in finite state model. So, the experimental value of this shift (-0.483 eV, Table 1) can b very accurately predicted in model where full hole screening on $2p$ -level is expected.

Somewhat another pattern is determined for atom $1d$. For it the experimental value of shift is 0.078 eV (Table 1). The

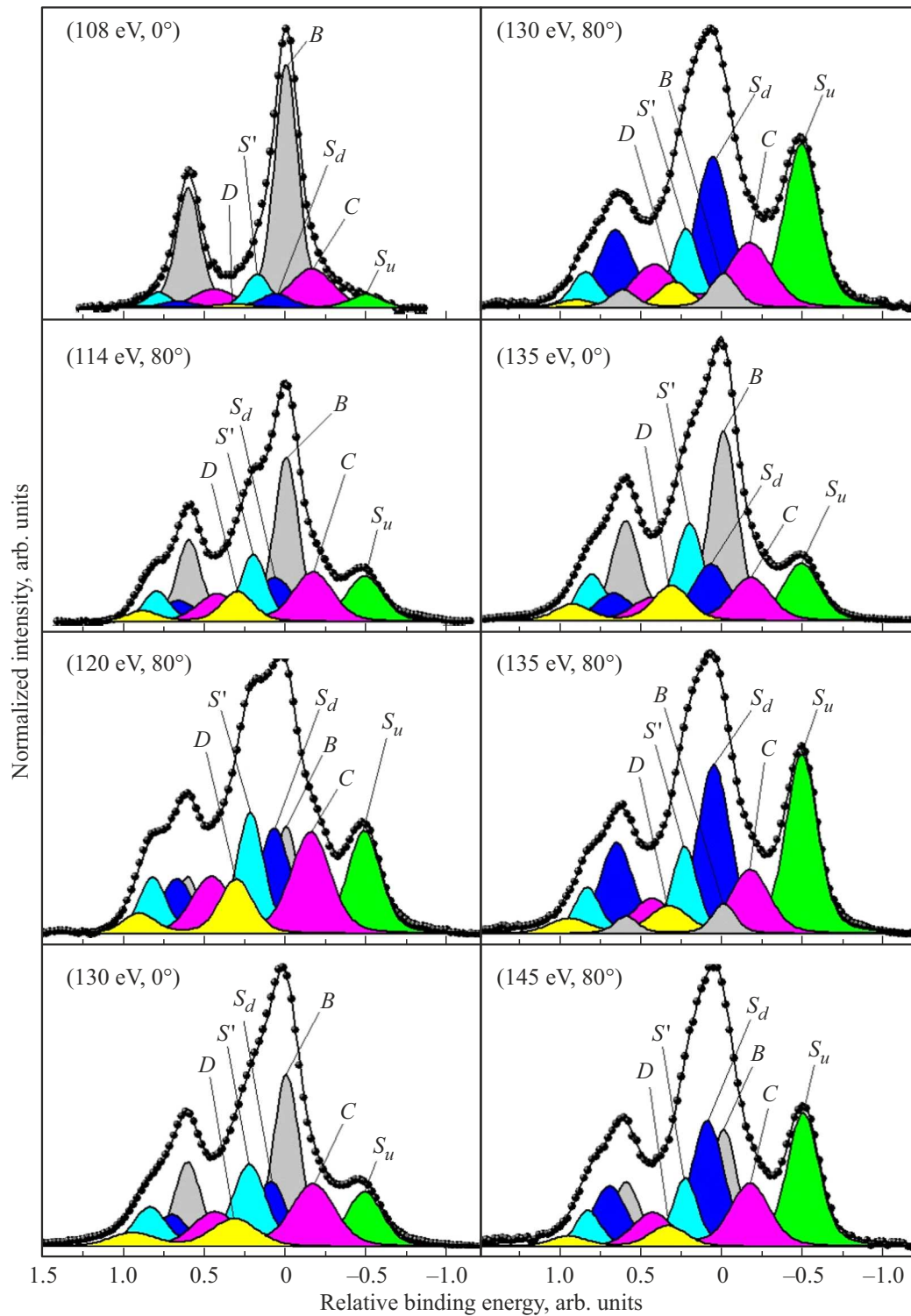


Figure 5. Decomposition of normalized Si $2p$ -spectra, obtained at different experimental conditions ($h\nu$, θ_e), to individual spin-orbit doublets. The bond energy along horizontal axis is read from position Si of $2p_{3/2}$ -sublayer of bulk component (B). For details see the text.

theory predicts value in range $0.41 - 0.57$ eV for initial state model and in range from -0.15 to 0.10 eV for the finite state model. This means that hole screening at $2p$ -level of atom $1d$ during electron emission into vacuum can be incomplete, or, in other words screening for atoms $1d$

occurs more slowly than for atoms $1u$. It can be supposed that this difference is associated with the features of the distribution of local electron density on the atoms of inclined dimers, which was already reported above. It is worth noting here that these results provide a clear example of

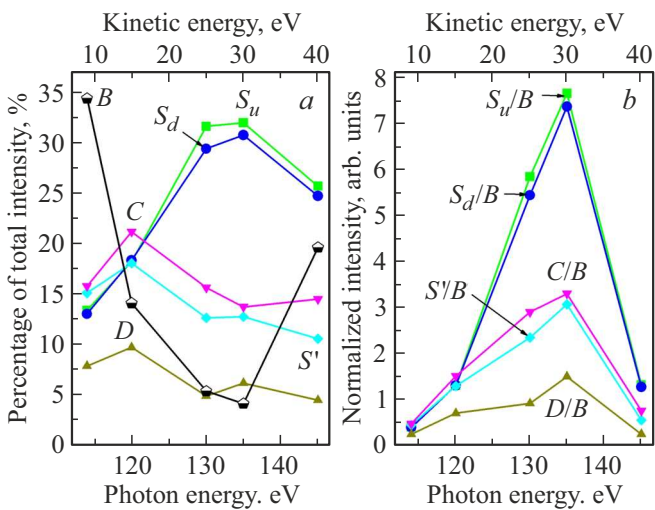


Figure 6. *a* — Contribution of components (in percents) to full intensity of $2p$ -spectra as function of photon energy. *b* — Normalized intensity of components S_u , S_d , S' , C and D vs. photon energy. Normalization was performed by value of bulk component. Emission angle $\theta_e = 80^\circ$.

the deep interrelationship between the geometric structure and the electronic properties of a solid: dimerization in the upper atomic layer of silicon in Figure 1 is accompanied not only by the energy splitting of the core $2p$ -level of atoms $1u$ and $1d$, but occurrence of difference in holes screening on their internal shells.

Atomic nature of components S' , C and D is less obvious. From Figure 6 it follows that their intensity depends much less sharply on the escape depth, and the largest contribution to the PE-line of the component S' , C and D is provided at $h\nu = 120$ eV (Figure 6, *a*). So, they can not be attributed neither to bulk lattice of silicon nor to atoms in its upper layer. We can suppose that these components are due to emission from atoms located under layer formed by atoms $1u$ and $1d$ in Figure 1. Number of such atoms can be evaluated from ratio of intensities of surface components in spectrum at $h\nu = 108$ eV and $\theta_e = 0^\circ$ in Figure 5. Under these conditions the electron escape depth is so high that the effects of signal attenuation from different surface layers in Figure 1 can be neglected. In this spectrum the ratio of areas of doublets ($S_u + S_d$), S' , C and D is 1 : 1 : 1.75 : 0.18. This means that components S' , C and D most likely are determined by the atoms of second, third and fourth layers. In Figure 1 this layers have six different atoms: 2, 3, 3', 4, 4' u and 4' d . Environment of some of them differs very insignificantly. Therefore, the surface shifts for such atoms can be quite close to each other and can not be completely resolved in the PE-spectra at 100 K and the current energy resolution. *Ab initio* calculations predict that the atoms of the second, third and fourth layers in Figure 1 give surface shifts in the range from -0.19 to 0.32 eV in initial state model [14,19,20] and in range from -0.26 to 0.27 eV in finite state model [11,14,19,20]. These shifts are

in reasonable agreement with the experimental values for S' and C in Table 1.

From all said above, it is logical to assume that the component S' occurs from atoms 2 in Figure 1, and component C is determined by atoms of third and fourth

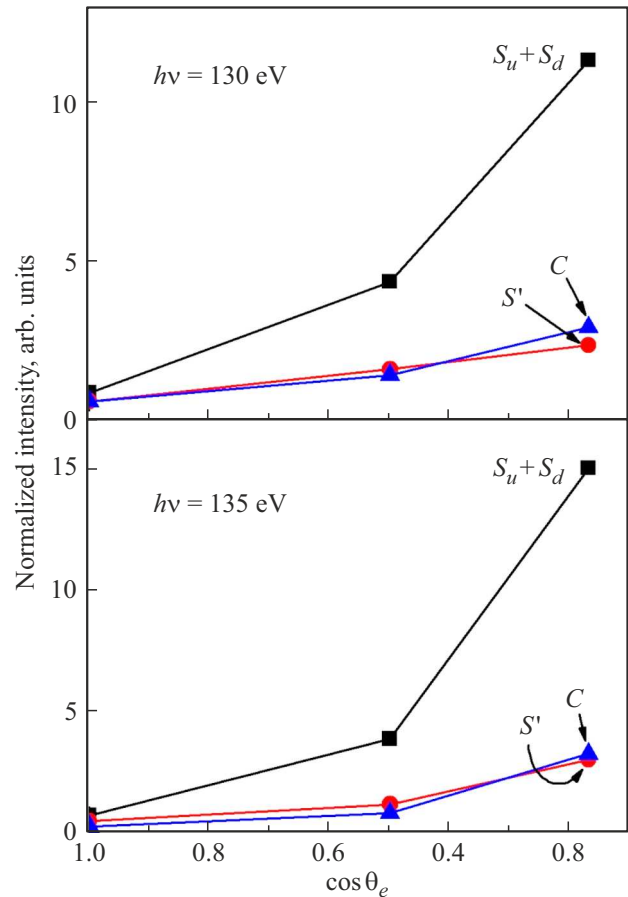


Figure 7. Normalized intensities ($S_u + S_d$), S' and C vs. escape angle cosine θ_e . Photon energy $h\nu$: *a* — 130 eV, *b* — 135 eV.

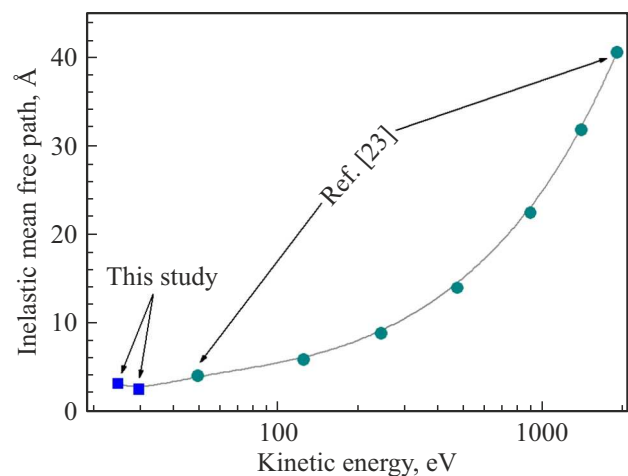


Figure 8. Mean free path of electron vs. kinetic energy in silicon. Data were obtained in present paper (square symbols) and in paper [23] (round symbols).

Table 2. Mean free path λ and escape depth $\lambda \cos \theta_e$, expressed in Å and in monolayers [ML] of silicon atoms, at different values $h\nu$ and θ_e

θ_e	$h\nu = 130 \text{ eV}$		$h\nu = 135 \text{ eV}$	
	λ (Å) [ML]	$\lambda \cos \theta_e$ (Å) [ML]	λ (Å) [ML]	$\lambda \cos \theta_e$ (Å) [ML]
0°	3.2 [2.4]	3.2 [2.4]	2.5 [1.8]	2.5 [1.8]
60°	3.2 [2.4]	1.6 [1.2]	2.6 [1.9]	1.3 [1.0]

layers in this reconstruction. This interpretation, firstly, agrees well with the intensity ratio of these components. Secondly, it is in agreement with the values of their Gaussian broadening in Table 1 (0.159 and 0.256 eV, respectively). As for D , the intensity of this component is very low to be uniquely associated with any type of atoms in the regular structure in Figure 1. The authors relate this component to the defects on surface of studied crystal. As it is known, such defects have natural origin and always form on smooth surfaces (100) of silicon to reduce surface tension [21,22].

Finally, results obtained in the present paper ensure evaluation of mean free path λ of electrons in silicon. Such evaluations were made for the kinetic energy of electrons 25 and 30 eV ($h\nu = 130$ and 135 eV). In Figure 7, *a* and 7, *b* for the above shown photon energies the dependences of normalized intensities ($S_u + S_d$), S' and C on escape angle cosine are shown. It was supposed that total intensity of components S_u and S_d is equal to value of PE-signal from first monolayer of silicon atoms, and total intensity of components S' and C corresponds to value of signal from second, third and fourth monolayers. The value 1.358 Å was taken as thickness of one monolayer of silicon atoms, it is equal to the height of a monoatomic step on Si(100) surface. The obtained results of value λ and escape depth $\lambda \cos \theta_e$ evaluation are given in Table 2 for cases $h\nu = 130$ and 135 eV and $\theta_e = 0^\circ$ and 60° . From it we see that at kinetic energy 30 eV ($h\nu = 135$ eV) the mean free path is low and is 2.55 Å (~ 1.9 of monolayer of silicon atoms). When the kinetic energy decreases to 25 eV the mean free path increases to 3.2 Å (2.4 of monolayer). In Figure 8 the obtained data are presented together with the results from paper [23]. It is evident that they are in good agreement and complement each other. The obtained values can be used to analyze the line shape in photoelectron spectroscopy of silicon surfaces.

4. Conclusion

The fine structure of $2p$ -spectra of high resolution was studied for surface Si(100) at 100 K in wide region of SC energies and escape angles. It is determined that the spectra include five surface components, four of which are due to emission from the atoms of the first (energy shifts -0.483 and 0.078 eV), second (0.225 eV), third and fourth (-0.163 eV) layer of reconstruction $c(4 \times 2)$. The fifth surface component (0.32 eV) is associated with defects

formed on surface. The optimal value of Lorentzian width ($\omega_L = 70$ meV) is obtained for these spectra decomposition. It is shown that they have maximum surface sensitivity at the photon energy 135 eV (kinetic energy of electrons ~ 30 eV). Based on the analysis of the intensities of surface components, the value of the electron mean free path in silicon crystal is determined as function of photon energy. At $h\nu = 135$ eV the mean free path is 2.55 Å, and at $h\nu = 130$ eV — 3.2 Å. These values are in good agreement with the published data.

Conflict of interest

The authors declare that they have no conflict of interest.

References

- [1] C.S. Fadley. Surf. Interface Anal. **40**, 1579 (2008).
- [2] D. Wolverson, B. Smith, E. Como, C. Sayers, G. Wan, L. Pasquali, M. Cattelan. J. Phys. Chem. C **126**, 9135 (2022).
- [3] Y. Kayser, C. Milne, P. Juranic, L. Sala, J. Czapla-Masztafiak, R. Follath, M. Kavcic, G. Knopp, J. Rehanek, W. Blachucki, M.G. Delcey, M. Lundberg, K. Tyrala, D. Zhu, R. Alonso-Mori, R. Abela, J. Sa, J. Szlachetko. Nature Commun. **10**, 4761 (2019).
- [4] M.V. Gomoyunova, I.I. Pronin. FTT **74**, 10, 1 (2004). (in Russian).
- [5] F.J. Himpsel, P. Heimann, T.-C. Chiang, D.E. Eastman. Phys. Rev. Lett. **45**, 1112 (1980).
- [6] G.K. Wertheim, D.M. Riffe, J.E. Rowe, P.H. Citrin. Phys. Rev. Lett. **67**, 120 (1991).
- [7] F.J. Himpsel, F.R. McFeely, A. Taleb-Ibrahimi, J.A. Yarmoff, G. Hollinger. Phys. Rev. B **38**, 6084 (1988).
- [8] D.H. Rich, T. Miller, T.-C. Chiang. Phys. Rev. B **37**, 3124 (1988).
- [9] D.-S. Lin, T. Miller, T.-C. Chiang. Phys. Rev. Lett. **67**, 2187 (1991).
- [10] E. Landemark, C.J. Karlsson, Y.-C. Chao, R.I.G. Uhrberg. Phys. Rev. Lett. **69**, 1588 (1992).
- [11] O.V. Yazyev, A. Pasquarello. Phys. Rev. Lett. **96**, 157601 (2006).
- [12] T.-W. Pi, C.-P. Cheng, I.-H. Hong. Surf. Sci. **418**, 113 (1998).
- [13] H. Koh, J.W. Kim, W.H. Choi, H.W. Yeom. Phys. Rev. B **67**, 073306 (2003).
- [14] P.E.J. Eriksson, R.I.G. Uhrberg. Phys. Rev. B. **81**, 125443 (2010).
- [15] D.A. Shirley. Phys. Rev. B **5**, 4709 (1972).

- [16] G.H. Major, N. Farley, P.M.A. Sherwood, M.R. Linford, J. Terry, V. Fernandez, K. Artyushkova. *J. Vac. Sci. Technol. A* **38**, 061203 (2020).
- [17] R.J. Hamers, R.M. Tromp, J.E. Demuth. *Phys. Rev. B* **34**, 5343 (1986).
- [18] R.A. Wolkov. *Phys. Rev. Lett.* **68**, 2636 (1992).
- [19] E. Pehlke, M. Scheffler. *Phys. Rev. Lett.* **71**, 2338 (1993).
- [20] M.P.J. Punkkinen, K. Kokko, L. Vitos, P. Laukkanen, E. Airiskallio, M. Ropo, M. Ahola-Tuomi, M. Kuzmin, I.J. Vayrynen, B. Johansson. *Phys. Rev. B* **77**, 245302 (2008).
- [21] R.M. Tromp, R.J. Hamers, J.E. Demuth. *Phys. Rev. Lett.* **55**, 1303 (1985).
- [22] B.S. Swartzentruber, Y.W. Mo, M.B. Webb, M.G. Lagally. *J. Vac. Sci. Technol. A* **7**, 2901 (1989).
- [23] C.J. Powell, A. Jablonski. *NIST Electron Inelastic-Mean-Free-Path Database*. Version 1.2, SRD 71. National Institute of Standards and Technology, Gaithersburg, MD (2010).

Translated by I.Mazurov